Investigating magnetic dynamo evolution with TESS field dwarfs

Of the measurable properties for a large ensemble of field stars, rotation periods contain the most information about stellar age, and provide the best leverage for advancing our knowledge of galactic archeology as well as exoplanet population demographics via gyrochronology. Angular momentum is carried away though magnetically driven stellar winds, which slows the star's rotation over cosmic time. This rotation-based 'clock' is known as gyrochronology. Cool spots on the star's surface rotate in-to and out-of view, creating small amplitude ($\pm$ 1%) quasi-periodic changes in the stellar brightness. Based on results from *Kepler*, using precise light curves available from the *TESS* mission, we expect to measure the rotation periods of around 20% of FG stars and 80% of KM stars in the Candidate Target List (CTL)[1]. For many of these stars it will be possible to infer an age from their rotation periods via gyrochronology.

Some outstanding mysteries regarding the nature of magnetic braking have been revealed, but thus-far unanswered by, *Kepler*. Firstly, a mysterious gap in the rotation period distribution of *Kepler* dwarfs requires either a sharp transition in magnetic dynamo geometry or a gap in the local star formation history as an explanation (McQuillan et al. 2014; Davenport 2017). Secondly, a transitioning magnetic dynamo appears to be responsible for inefficient magnetic braking at old ages in Solar-mass stars. **We propose to help answer these questions by providing a catalog of rotation periods for *TESS* Full Frame Image (FFI) stars.**

Scientific Justification The bimodal period distribution among field stars discovered by McQuillan et al. (2013), is shown in Figure 1. Recently, Co-I Davenport discovered this period bimodality extends throughout all masses in the Kepler rotation sample for nearby stars (Davenport 2017). This feature could either reflect a drop in the star formation rate around 600 Myr ago or could be explained by a previously unknown variation in the spin-down evolution for low-mass stars. The TESS FFI and CTL targets will provide the ideal dataset to test these two scenarios explaining the appearance of a period bimodality. If the bimodal period distribution reflects a discontinuous age distribution, the feature should be local and may disappear at greater distances or along different lines of sight. However, if the bimodality is truly due to a transition point in the spin-down evolution at young ages, there should be little to no variation in the feature with galactic position. We will match the TESS FFI and CTL targets to the upcoming data release from the Gaia mission (Perryman et al. 2001) to map the rotation period distribution as a function of galactocentric position. For the all-sky analysis we will focus on F and G stars since the 27.5 day baseline of *TESS* fields will limit measureable rotation periods to less than around 15 days. With the April 2018 data release from Gaia (DR2), we estimate that we will be able to study rotation periods for G dwarfs in the TESS FFIs out to $\sim$3 kpc. To characterize the rotation period bimodality as a function of galactic position, we propose to analyse the light curves of 10,000 FFI and

[1] The difference between these percentages comes from a dramatic increase in magnetic activity towards lower masses.

two-minute targets that overlap with the Tycho-Gaia Astrometric Solution (TGAS) catalog, selecting FGKM dwarfs with a range of galactic positions. The FFI targets will be essential in order to reach ∼3kpc distances. M dwarfs rotation periods in the CVZz will allow us to study the rotation period bimodality at lower masses, since the bimodality appears at longer rotation periods for lower mass stars. Unlike *Kepler* and *K2* light curves, *TESS* provides the all-sky coverage necessary to map the period bimodality across the galaxy.

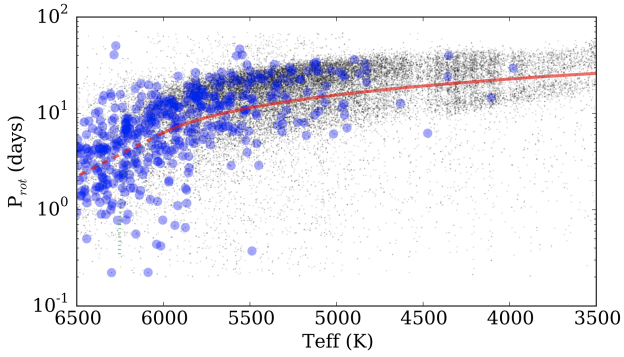

Fig. 1.— From Davenport (2017). Rotation period as a function of effective temperature for the full McQuillan et al., (2014) Kepler sample in black, and the subset of these stars that also feature in the TGAS Gaia DR1 catalogue in blue. Contaminating giants have been removed from the blue sample and the rotation period bimodality is revealed to exist across all temperatures shown. The red line is a 600 Myr rotational isochrone (also known as a gyrochrone).

Although the classical spin-down law of Skumanich (1972): Period $\propto$ Age^1/2 holds for all open clusters with measured periods, it does not appear to describe old field stars (Angus et al. 2015; van Saders et al. 2016). van Saders et al. (2016) found that including a transition to a weakened magnetic braking regime in the gyrochronology models, at a critical Rossby number, provides an improved fit to the data. Further calibration is needed however; a lack of rotation periods and reliable ages for old and low-mass stars leaves the rotational evolution of stars older than the Sun relatively unexplored. *TESS* will provide thousands of new rotation periods for both FFI and two-minute cadence stars, with the maximum measurable period strongly depending on the length of time it is observed for. Of particular interest are the potentially long rotation periods measurable for stars that fall in the Continuous Viewing Zones (CVZs). Many of these will have spectra from the *TESS–HERMES* survey, from which it will be possible to calculate isochronal ages, enabling further calibration of the gyrochronology relations. We will also use the rotation periods of TESS field dwarfs over the whole sky to test the gyrochronology relations using galactic kinematics. Many stars observable by *TESS* will have proper motions, parallaxes, positions and radial velocities published in the second *Gaia* data release. These parameters provide the information necessary to calculate galactocentric positions and action angles of the stars, both of which are age indicators. Since one of the few ways to accurately age-date fully convective, late M dwarfs is via kinematics, these new relations will help to infer ages for all stars with M$<$ 0.35M$_\odot$, to which gyrochronology cannot be applied.

In addition, we will use the rotation periods of comoving stars identified in the first *Gaia* data release (Oh et al. 2016) to quantify the accuracy and precision of gyrochronology. We have identified 38 stars in 19 pairs with *Gaia* proper motions and radial velocities from *RAVE* that are observable by *TESS*, using `tvguide`. Of these, 34 stars in 17 pairs are already in the CTL list. Because the stars in these pairs are assumed to be recently disrupted binaries,

we expect them to have the same age and measuring their rotation periods will therefore provide a test of gyrochronology.

Technical Feasibility The extraction of a rotation period from a light curve can be as simple as computing a Lomb-Scargle periodogram or, in cases where the signal is less clear, can be inferred via modeling the correlation between data points. This latter approach could involve either computing an autocorrelation function (McQuillan et al. 2013), or fitting a Gaussian process to the time series (Angus et al. 2017; Foreman-Mackey et al. 2017b). In cases where signals have long periods and low amplitudes, care is needed to separate real astrophysical signal from instrumental systematics. The measurement of rotation periods is less sensitive to crowding and source confusion than exoplanet transit characterization because the rotation period is not effected by photometric dilution. We will apply two complementary methods to extract and calibrate light curves from the TESS FFIs. First, for bright or isolated targets, we will follow Montet et al. (2017) to estimate aperture shapes and perform aperture photometry for bright sources. Using an ensemble of sources, we will de-trend these light curves using a modified version of everest (Luger et al. 2016, 2017) designed to preserve photometric signatures of rotation. This will be achieved by fitting for the systematic effects in the light curve using the everest model simultaneously with a Gaussian Process model for the astrophysical variation. Both Aigrain et al. (2016) and Luger et al. (2016) demonstrated that this can preserve stellar variability signals and we will use the celerite algorithm (Foreman-Mackey et al. 2017a) to scale the computations to the size of TESS FFI datasets. The precision of existing photometric de-trending methods degrades in crowded fields (for example, Luger et al. 2017). However, to make robust measurements of rotation periods, we do not need absolutely calibrated light curves. Therefore, in crowded fields, we will apply a difference imaging method that was developed for the K2 Campaign 9 microlensing project (Henderson et al. 2016) based on the CPM (Wang et al. 2016) to robustly measure the photometric variations of crowded sources. Unlike standard difference imaging methods, this procedure does not require a reference image. Instead, a causal data-driven model is built to predict the time series in every pixel taking systematic effects into account and the residuals between the observations and the model predictions provide an estimate of the astrophysical variability in each pixel. We will tune this method preserve rotation signals and apply it to detect rotation across the FFIs.

The full set of available *TESS* FFI and two-minute cadence light curves will be exceedingly large and we intend to prioritize certain groups of stars for period analysis, calculating a simple (and computationally fast) Lomb-Scargle periodogram for the low priority objects and running a full probabilistic period analysis on the high priority targets. High priority targets include: comoving pairs, stars in the CVZs (especially those with spectra), stars in TGAS, stars at large distances, plus any potential asteroseismic dwarfs and exoplanet hosts. Based on the expected photometric precision of *TESS* (Sullivan et al. 2015), we expect to be able to measure rotation periods for stars down to 16th magnitude in the FFIs. We note, however that not all stars will have measurable rotation periods, even if they are bright

enough — not all stars show rotational variability in their light curves either because they are pole-on or because they are inactive.

We have already begun to construct a rotation period catalog of *K2* stars, for which we have received funding from the Archival Data Analysis Program (ADAP). Figure 2 shows a map of preliminary rotation periods for one of four *K2* fields processed so far.

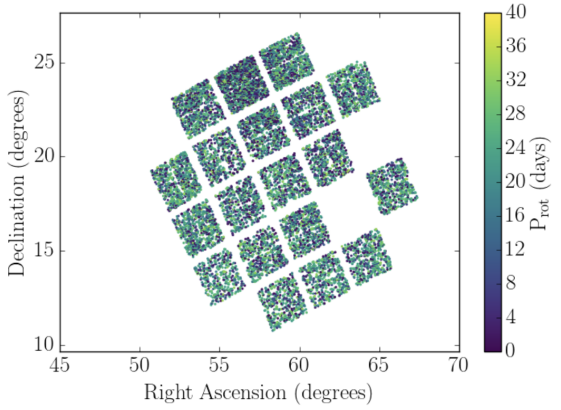

Fig. 2.— All stars observed during K2 campaign 4, plotted according to their equatorial coordinates and colored by their preliminary rotation period. These rotation periods were measured using a simple ACF method, applied to everest (Luger et al., 2015) light curves.

Expected Impact Initially we will provide rotation period posterior probability density functions and best fit estimates for around 30,000 high priority two-minute cadence and FFI targets. We will then produce a catalog of rotation periods for lower priority stars using a combination of Lomb-Scargle periodogram and autocorrelation techniques. Finally, we will release a catalog of rotation periods for two-minute cadence targets. We will also release an open source python package for measuring rotation periods of both FFI and two-minute cadence targets.

Budget Justification PI Angus intends to use the budget to employ a student for 3-4 months. In this time the student will assist in extracting light curves from the FFIs, measuring rotation periods and building a rotation period catalog. The student will also be involved in the scientific project of their choosing: either the rotation period bimodality, gyrochronology of low-mass stars, or gyrochronology of comoving pairs. The remaining budget will be used for traveling to meet with other Co-Is in order to perform this analysis.

References

Aigrain, S., Parviainen, H., & Pope, B. J. S. 2016, MNRAS, 459, 2408

Angus, R., Aigrain, S., Foreman-Mackey, D., & McQuillan, A. 2015, MNRAS, 450, 1787

Angus, R., Morton, T., Aigrain, S., Foreman-Mackey, D., & Rajpaul, V. 2017, ArXiv e-prints, arXiv:1706.05459

Davenport, J. R. A. 2017, ApJ, 835, 16

Foreman-Mackey, D., Agol, E., Ambikasaran, S., & Angus, R. 2017a, ArXiv e-prints, arXiv:1703.09710

Foreman-Mackey, D., Agol, E., Angus, R., & Ambikasaran, S. 2017b, ArXiv e-prints, arXiv:1703.09710

Henderson, C. B., Poleski, R., Penny, M., et al. 2016, PASP, 128, 124401

Luger, R., Agol, E., Kruse, E., et al. 2016, AJ, 152, 100

Luger, R., Kruse, E., Foreman-Mackey, D., Agol, E., & Saunders, N. 2017, ArXiv e-prints, arXiv:1702.05488

McQuillan, A., Aigrain, S., & Mazeh, T. 2013, MNRAS, 432, 1203

McQuillan, A., Mazeh, T., & Aigrain, S. 2014, ApJS, 211, 24

Montet, B. T., Tovar, G., & Foreman-Mackey, D. 2017, ArXiv e-prints, arXiv:1705.07928

Oh, S., Price-Whelan, A. M., Hogg, D. W., Morton, T. D., & Spergel, D. N. 2016, ArXiv e-prints, arXiv:1612.02440

Perryman, M. A. C., de Boer, K. S., Gilmore, G., et al. 2001, A&A, 369, 339

Skumanich, A. 1972, ApJ, 171, 565

Sullivan, P. W., Winn, J. N., Berta-Thompson, Z. K., et al. 2015, ApJ, 809, 77

van Saders, J. L., Ceillier, T., Metcalfe, T. S., et al. 2016, Nature, 529, 181

Wang, D., Hogg, D. W., Foreman-Mackey, D., & Schölkopf, B. 2016, PASP, 128, 094503